

# Electrochemical and spectroscopic characterization of the interaction between DNA and Cu(II)–naringin complex

Lucilene D. Mello<sup>a</sup>, Regina M.S. Pereira<sup>b</sup>, Alexandra C.H.F. Sawaya<sup>a,b</sup>,  
Marcos N. Eberlin<sup>a</sup>, Lauro T. Kubota<sup>a,\*</sup>

<sup>a</sup> Instituto de Química, UNICAMP, P.O. Box 6154, 13083-970 Campinas, SP, Brazil

<sup>b</sup> UNIBAN, Rua Maria Cândida, 1813 Vila Guilherme, São Paulo, SP, Brazil

Received 20 March 2007; received in revised form 6 August 2007; accepted 8 August 2007

Available online 14 August 2007

## Abstract

In this work the interaction of DNA and the flavonoid–transition metal complex (Cu(II)–naringin complex) is characterized. The interaction was evaluated by using electrochemical ssDNA- and dsDNA-based biosensors and the results were supported by UV, CD and <sup>1</sup>H NMR data. In the electrochemical method, changes in the oxidation peak of the guanine and adenine bases obtained by square wave voltammetry (SWV) showed evidence of the interaction. The variations of the spectroscopic characteristics of DNA and Cu(II)–naringin complex in aqueous medium demonstrated that the predominant interaction mode may be by intercalation. Cu(II)–naringin complex interacts to dsDNA probably via N(7) of guanine site.

© 2007 Elsevier B.V. All rights reserved.

**Keywords:** DNA biosensor; Screen-printed electrode; SWV; Copper-naringin complex; Spectroscopy

## 1. Introduction

DNA plays a key role in the synthesis of proteins (gene expression) as well as its own replication making it a potential target for drugs, especially for antiviral, antibiotic and anticancer action. Thus, favorable DNA interaction patterns based on the study of small molecules that bind to nucleic acids is one of the most important parameters in the screening design for new drugs and development processes. The recognition of the DNA binders involves a complex interplay of a variety of interactive forces. It includes hydrogen bonding interactions, strong electrostatic interactions arising due to phosphates, mobile counter-ions, hydration and Van der Waals interactions [1]. As a result, the formed DNA–drug complex leads to changes in the thermodynamic stability and structural properties of DNA.

In this context, there is a constant interest to find and to characterize new substances that can exert some biological and biochemical effects as anticancer or antibiotic drugs. The clinical use of drugs is limited by some factors such as the limited

spectrum of their anticancer activity, development of resistance after continuous treatment and another very important aspect is that frequently these compounds are highly toxic to normal cells [2].

Recently, natural substances such as flavonoids, that show biological activity in many mammalian cell systems *in vitro* and *in vivo*, have been investigated as to their interaction with DNA. Association studies reported with DNA involving flavonols such as morin [3], quercetin [4], kaempferide and luteolin [5] revealed that the predominant interaction mode is intercalative. Some works obtained with resveratrol and genistein [6,7] have confirmed that their structural configuration, possessing a planar aromatic system, is suitable to insert between base-pairs in a helix. Most flavonoids have a common phenyl–benzopyrone skeleton, which differ with respect to the hydroxyl and methoxy groups (Fig. 1). Their nucleophilic structure in the chromophore region, which includes the B-ring, the 2,3 double bond and the carbonylic region, justify their notable antioxidant activity due to the free radical scavenging abilities and metal complexing agents [8].

In contrast to the accepted protective role of the flavonoids, literature evidences the action of these compounds in mutagenic process [9,10] and having DNA damaging ability [11,12].

\* Corresponding author. Tel.: +55 1935213127; fax: +55 1935213023.

E-mail address: [kubota@iqm.unicamp.br](mailto:kubota@iqm.unicamp.br) (L.T. Kubota).

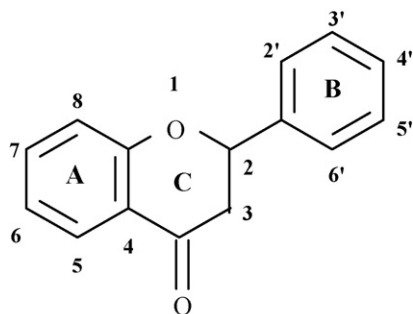


Fig. 1. Basic structure of flavonoids.

Others work reveal that the strand scission of the DNA by flavonoids is increased in the presence of transition metal ions, such as copper(II) and iron(II) [13,14]. Previously, other studies showed that the nuclease ability is more active when the polyphenol is modified forming flavonoid–transition metal complexes [8]. This behavior can be associated to the mode of interaction with DNA. The energy of the intercalating mode of binding causes a structural perturbation and leads to cell cycle arrest and DNA degradation. In fact, each flavonoid has a particular structure, which possibly has different binding modes and each mode resulting in a characteristic distortion of the DNA, this in theory gives rise to a specific pharmacological effect.

In this direction, research to understand how flavonoid compounds interact with biomarkers, like DNA are important to obtain information about their therapeutic potential, considering that these substances are present in plants in high concentrations and are identified as active principles in most of them. For this purpose, the use of electrochemical and spectroscopic methods applied to a drug–DNA interaction system *in vitro* provide a useful complement to other methods and in many cases yield information about the interaction mechanism.

The class of affinity biosensor consisting of nucleic acid layers combined with electrochemical transducer has been found suitable in the detection of genotoxic substances. It has also shown a great potential in drug–biological target interaction studies, in special those related to the cancer chemotherapy where DNA is the main marker [1,15]. Thus, DNA-based biosensor can be used as an efficient screening system to discover new drugs.

Information about the mechanism of interaction between a flavonoid–transition metal complex, Cu(II)–naringin complex and DNA is the main aim of this work. An electrochemical DNA-based biosensor and UV, CD and  $^1\text{H}$  NMR spectroscopic methods were employed during the investigation.

## 2. Experimental

### 2.1. Reagents and solutions

Nucleotide 5'GMP, copper acetate, sodium acetate, sodium chloride, naringin and chromatographic grade methanol were purchased from Merck (Darmstadt, Germany). Lyophilized single (ssDNA D8899) and double (dsDNA D4522) stranded

calf thymus DNA was supplied by Sigma (St. Louis, USA). All aqueous solutions were prepared using ultrapure water ( $\rho > 18 \text{ M}\Omega \text{ cm}^{-1}$ ) from a Milli-Q system (Millipore, System). DNA stock solutions (nominally  $1000 \text{ mg L}^{-1}$ ) were prepared in purified water, taking aliquots and storing in a freezer. The screen-printed electrodes were obtained from Prof. Marco Mascini Laboratory (Florence, Italy).

### 2.2. Synthesis of the Cu(II)–naringin complex

The synthesis of the complex consisted in the preparation of an aqueous solution of copper acetate(II)  $[\text{Cu}(\text{CH}_3\text{COO})_2]$   $1.25 \times 10^{-4} \text{ mol}$  (0.0249 g) in 2 mL of distilled/purified water and dropped slowly in a methanol solution of naringin  $2.5 \times 10^{-4} \text{ mol}$  (0.146 g in 10 mL methanol). The mixture was stirred for 30 min at room temperature. The precipitate was filtered in a vacuum system, washed with water and dried by liofilization. The resulting compound 0.0595 g of Cu(II)–naringin complex was obtained (60% yield). %C (calc); %H (calc) for  $\text{CuC}_{29}\text{H}_{46}\text{O}_{21}$ : 42.50 (42.98); 5.22 (5.68).

Melting point of naringin ( $171^\circ\text{C}$ ) and Cu(II)–naringin complex ( $242^\circ\text{C}$ ) were obtained in Quimus Melting Point Equipment.

### 2.3. Spectroscopic characterization of the Cu(II)–naringin complex

The Cu(II)–naringin complex was characterized by FT-IR, UV–vis and  $^1\text{H}$  NMR spectroscopy and mass spectrometry techniques.

Infrared measurements were recorded in KBr pellets in  $4000\text{--}400 \text{ cm}^{-1}$  range using a FT-IR Nexus spectrophotometer. The UV–vis spectra were recorded in methanol solution in  $600\text{--}200 \text{ nm}$  range using a Varian Cary 50 spectrophotometer.

In the mass spectrometry characterization, the samples were analyzed by direct infusion electrospray ionization (ESI) by means of a syringe pump (Harvard Apparatus) at a flow rate of  $10 \mu\text{L min}^{-1}$ . Positive ion mode ESI-MS fingerprints and positive mode ESI-MS/MS for collision-induced dissociation (CID) were acquired using a hybrid high-resolution and high-accuracy (5 ppm) Micromass Q-TOF mass spectrometer (Micromass UK Ltd., Manchester, UK). Capillary and cone voltages were set to 3000 V and 30 V, respectively, with a desolvation temperature of  $100^\circ\text{C}$ . Samples were added to a solution containing 70% (v/v) chromatographic grade methanol (Tedia, Fairfield, OH, USA) and 30% (v/v) deionized water and  $1 \mu\text{L}$  of formic acid (Merck, Darmstadt, Germany) per millilitre. Fingerprint mass spectra were acquired in the range between  $m/z$  100 and 2000 where no ions attributed to the solvents used were observed.

$^1\text{H}$  NMR spectra were recorded at room temperature with a Varian Gemini-2000 NMR spectrometer operating at frequency of 300 MHz using 3-(trimethylsilyl)-propanesulfonic acid sodium salt ( $\text{D}_2\text{O}$ ) (Merck, 99.8% D) or DMSO (Merck) as solvent. All chemical shifts ( $\delta$ ) of protons were measured in relation to the residual peak of the solvent and given in parts per million.

## 2.4. Measurements for characterization of the DNA–complex interaction

The interaction between DNA and Cu(II)–naringin complex was characterized by UV–vis, CD and  $^1\text{H}$  NMR spectroscopy techniques.

The UV absorption spectra recorded in acetate buffer  $0.25\text{ mol L}^{-1}$  (pH 5.0) were obtained in a UV–vis spectrophotometer from Pharmacia Biotech<sup>®</sup> Ultrospec 2000 connected to a PC (software Wavescan<sup>®</sup>) using a quartz cuvette (10 mm path length).

Circular dichroism (CD) spectra were obtained in acetate buffer  $0.25\text{ mol L}^{-1}$  (pH 5.0) at room temperature by using a JASCO J-180 spectropolarimeter (JASCO Co. Ltd., Hachioji, Japan) in a quartz cell (10 mm path length) using a computer for spectral subtraction and noise reduction. Each CD spectrum was collected by taking the average of at least three accumulations using a scan speed of  $50\text{ nm min}^{-1}$  and response time of 3 s with 1 nm intervals from 210 to 320 nm.

$^1\text{H}$  NMR measurements were carried out in the same conditions and apparatus used for characterization of the Cu(II)–naringin complex. The concentration of 5'GMP and Cu(II)–naringin complex solutions were  $5.1 \times 10^{-5}\text{ mol L}^{-1}$  and  $1.8 \times 10^{-5}\text{ mol L}^{-1}$ , respectively.

## 2.5. Electrochemical measurements and apparatus

### 2.5.1. Biosensor preparation

The biosensor preparation procedure consisted in a clean step of the electrode before the DNA immobilization. The electrode surface was treated by applying a fixed potential of +1.6 V for 2 min, after applying +1.8 V for 3 min in acetate buffer ( $0.25\text{ mol L}^{-1}$ , pH 4.7 containing  $10\text{ mmol L}^{-1}$  of sodium chloride), versus Ag pseudo-reference electrode. The initial conditioning step improves the resolution of the analytical signal because the application of high potentials in acidic medium increases the hydrophilic properties of the electrode surface through the introduction of oxygenated functionalities [16]. The ssDNA and dsDNA were subsequently immobilized onto the activated electrode surface by adsorptive accumulation involving the application of positive electrode potential to achieve electrostatic binding of negatively charged DNA. Thus, the electrode was immersed in an acetate buffer containing DNA from calf thymus and it was applied a potential of +0.5 V versus Ag-pseudo-reference electrode, for 5 min.

Differences among screen-printed electrodes used as disposable were recorded by using the normalized (relative) signal  $I_{\text{pDNAbound}}/I_{\text{pDNAfree}}$ , for the same electrode and it is referred as DNA signal in the text. This was recorded in the following steps: (a) DNA-free signal ( $I_{\text{pDNAfree}}$ ) expressed as the DNA signal recorded in acetate buffer only; (b) DNA bound ( $I_{\text{pDNAbound}}$ ) expressed as the DNA signal recorded in acetate buffer after interaction with the complex. All signals were recorded after applying the electrochemical conditioning step of the electrode surface followed by the DNA immobilization step as described earlier.

### 2.5.2. Electrochemical measurements

Measurements were carried out at room temperature and using a screen-printed electrochemical cell based on a silver pseudo-reference electrode, graphite working electrode and graphite as auxiliary electrode. Each electrode was used as disposable. A potentiostat Autolab<sup>®</sup> PGSTAT30 connected to a PC (software GPES 4.8) from Eco Chemie (The Netherlands) was employed in the electrochemical measurements. The interaction between DNA and Cu(II)–naringin complex in acetate buffer was investigated by using square wave voltammetry (SWV). The experimental parameters were: potential range between +0.2 and 1.5 V; frequency = 200 Hz; step potential = 15 mV; amplitude = 40 mV. All measurements were carried out under stirred solution. In the data treatment process, the original signals were recorded using the Autolab<sup>®</sup> software and applied Savitzky and Golay filter (level 2) with moving average baseline correction (peak width = 0.05).

## 3. Results and discussion

### 3.1. Characterization of the Cu(II)–naringin complex

The Cu(II)–naringin complex was characterized by FT-IR and UV–vis spectroscopy. Naringin shows a maximum absorption, in methanol solution, at 282 nm attributed to the A ring portion and a very weak band at 326 nm, attributed to the B ring portion. Upon binding with Cu(II), the maximum absorption band shifted to 304 nm and the weak band shifted to 379 nm, a considerable shift in relation to uncomplexed flavonoid. This change in the maximum absorption suggested an interaction of the Cu(II) ion with the condensed ring of the flavonone in the positions 4 and 5 [17,18].

The infrared spectra of free naringin in KBr pellets showed bands at  $1645\text{ cm}^{-1}$  ( $\nu_{\text{CO}}$ ) and  $1298\text{ cm}^{-1}$  ( $\nu_{\text{C-O-C}}$ ). Upon binding to Cu(II), the complex exhibits bands at  $1614\text{ cm}^{-1}$  ( $\nu_{\text{CO}}$ ) and  $1274\text{ cm}^{-1}$  ( $\nu_{\text{C-O-C}}$ ), which indicates the coordination of the copper to the condensed ring of naringin.

Complexation of Cu(II) to naringin was also verified by  $^1\text{H}$  NMR, but using DMSO- $d_6$  as a solvent. The peak of the naringin and Cu(II)–naringin complex in the  $^1\text{H}$  NMR spectra are shown in Table 1. The spectra of naringin is compared with the spectra of the complex and significant differences between the spectra a shift of the signals of the H<sub>6</sub>; H<sub>8</sub>, H<sub>2'</sub>; H<sub>6'</sub> H<sub>3'</sub>; H<sub>5'</sub>, H<sub>2</sub> and H<sub>3</sub> are observed. The proton signals of the complex are shifted to low frequency relative to the free flavonoid, due to coordination with copper ion, which decreases the electron density of the flavonoid. The signal referent to H<sub>2</sub> and H<sub>3A</sub> and H<sub>3B</sub> in complex becomes broader when compared to free naringin. This coordination could increase the planarity of the flavonoid, therefore decreasing the mobility of the protons and as a result broadening the signals.

In order to obtain more structural information of the Cu(II)–naringin complex, mass spectrometry data were also obtained. The positive ion mode ESI-MS fingerprint of the complex sample showed characteristic ions with nominal  $m/z$  581, 603, 619, 641, 643, 673, 675, 705, 707, 796, 798, 889, 933, 1183 and 1222. These ions were mass selected and submitted to

Table 1  
Partial data of  $^1\text{H}$  and  $^{13}\text{C}\{^1\text{H}\}$  NMR for the naringin and Cu(II)–naringin complex

| Compound                | $^1\text{H}$ NMR ( $\delta$ , ppm)  |
|-------------------------|---|
| Naringin                | 11.88 (s, OH); 9.51 (s, OH); 7.17 (d, $\text{H}_{2'}$ , $\text{H}_{6'}$ , $J=8.0$ Hz); 6.64 (d, $\text{H}_{3'}$ , $\text{H}_{5'}$ , $J=8.0$ Hz); 5.94 (d, $\text{H}_8$ , $J_{\text{H}_6/\text{H}_8}=7.0$ Hz); 4.97 (d, $\text{H}_6$ , $J_{\text{H}_6/\text{H}_8}=7.0$ Hz); 5.13 (dd, $\text{H}_2$ , $J_{\text{H}_2-\text{H}_{3\text{A}}}=4.5$ Hz and $J_{\text{H}_2-\text{H}_3}=3.0$ Hz); 4.70 (dd, $\text{H}_{3\text{A}}$ , $J_{\text{H}_{3\text{A}}-\text{H}_{3\text{B}}}=12.0$ Hz and $J_{\text{H}_2-\text{H}_{3\text{A}}}=4.5$ Hz); 4.8 (dd, $\text{H}_{3\text{B}}$ , $J_{\text{H}_{3\text{A}}-\text{H}_{3\text{B}}}=12.0$ Hz and $J_{\text{H}_2-\text{H}_{3\text{A}}}=3.0$ Hz) |
| Cu(II)–naringin Complex | 12.05 (s, 1H, 5-OH); 9.64 (s, 4'-OH); 7.02 (d, $\text{H}_{2'}$ , $\text{H}_{6'}$ , $J=6.6$ Hz); 6.52 (d, $\text{H}_{3'}$ , $\text{H}_{5'}$ , $J=7.0$ Hz); 5.78 ( $\text{H}_8$ , $J_{\text{H}_6/\text{H}_8}=5.5$ Hz); 4.79 (Sbr); 5.13 (m, $\text{H}_2$ ), 4.70 (dd br, $\text{H}_{3\text{A}}$ , $J_{\text{H}_{3\text{A}}-\text{H}_{3\text{B}}}=12.0$ Hz and $J_{\text{H}_2-\text{H}_{3\text{A}}}=4.5$ Hz); 4.8 (dd br, $\text{H}_{3\text{B}}$ , $J_{\text{H}_{3\text{A}}-\text{H}_{3\text{B}}}=12.0$ Hz and $J_{\text{H}_2-\text{H}_{3\text{A}}}=3.0$ Hz)   |

collision-induced dissociation (CID) in order to elucidate their structures. The identified structures can be observed in Table 2.

These results suggest that naringin molecule interacts with Cu(II) by losing a hydrogen and co-coordinating preferentially with two molecules of methanol per Cu(II) and having a counterions (lost during ionization) observed as  $m/z$  705 and 707. During the ionization, the methanol adducts are sometimes lost, observed as  $m/z$  641, 643, 673 and 675. Adducts of naringin with sodium and potassium were also observed, as these elements are commonly found in natural products as well as protonated naringin, observed as  $m/z$  603, 619 and 581, respectively. These are probably present in small proportions but ionize well in the positive ion mode. Clusters containing two or more molecules of naringin are also probably present in solution and can be observed as  $m/z$  933, 1183 and 1222.

The elemental analysis shows experimental data, %C 42.50 and %H 5.22, what suggested a proportion of 1:1 of Cu(II) ion/naringin. Therefore, in solid state as  $[\text{Cu}(\text{naringin})]^+[\text{CH}_3\text{COO}]^- \cdot 5\text{H}_2\text{O}$  can be proposed. When dissolved in methanol, it coordinates with two molecules of solvent, leading to square planar geometry with  $\text{CH}_3\text{COO}^-$  as counterion (Fig. 2b) [19].

Table 2  
Nominal  $m/z$  of ions observed in the positive ion mode ESI-MS fingerprint of the Cu/naringin sample and identified structures

| Nominal, $m/z$ | Identified structure   |
|----------------|--|
| 581            | $[\text{Naringin} + \text{H}]^+$   |
| 603            | $[\text{Naringin} + \text{Na}]^+$  |
| 619            | $[\text{Naringin} + \text{K}]^+$   |
| 641            | $[\text{Naringin}-\text{H} + ^{63}\text{Cu}]^+$  |
| 643            | $[\text{Naringin}-\text{H} + ^{65}\text{Cu}]^+$  |
| 673            | $[\text{Naringin}-\text{H} + ^{63}\text{Cu} + \text{CH}_3\text{OH}]^+$                       |
| 675            | $[\text{Naringin}-\text{H} + ^{65}\text{Cu} + \text{CH}_3\text{OH}]^+$                       |
| 705            | $[\text{Naringin}-\text{H} + ^{63}\text{Cu} + 2\text{CH}_3\text{OH}]^+$                      |
| 707            | $[\text{Naringin}-\text{H} + ^{65}\text{Cu} + 2\text{CH}_3\text{OH}]^+$                      |
| 933            | Doubly charged: $[3 \text{Naringin}-2\text{H} + 2 ^{63}\text{Cu}]^{2+}$                      |
| 1183           | $[2 \text{Naringin} + \text{Na}]^+$  |
| 1222           | Doubly charged: $[4 \text{Naringin}-2\text{H} + ^{63}\text{Cu} + \text{Na} + \text{K}]^{2+}$ |

According to the FT-IR, UV–vis and the mass spectrometry analysis, the proposed structure of the complex can be observed in Fig. 2b.

In the solution, a square planar configuration was proposed, containing one copper ion coordinating with naringin probably through the carbonyl group in position 4 and by oxygen of hydroxyl group in position 5 and two methanol molecules (Fig. 2b).

### 3.2. Electrochemical characterization of the interaction

In the characterization of the interaction, some preliminary observation were important such as: the Cu(II)–naringin complex interaction with DNA, the free naringin compound not binding with the macromolecule. It was also observed the Cu(II)–naringin complex showed no electrochemistry activity when tested using a KCl 0.1 mol L $^{-1}$  solution as electrolyte in the studied potential range.

Thus, the study was carried out considering the system involved basically three important steps: (I) DNA-based biosensor preparation; (II) interaction of the complex with the biosensor and (III) evaluation of the event that occurred at electrode surface.

The DNA-based biosensor preparation procedure (step of pretreatment of the electrode surface and DNA immobilization) as well as the general assay conditions (buffer composition, ionic strength, pH, electrochemical method and parameters of measurements) was reported in a previous work [20].

Thus, the interaction study was accompanied by changes in the electrochemical signals of the DNA bases, in special, the guanine peak. Guanine (G) is one of the two main purine bases present in nucleic acids, with the smallest (among the other bases) value of redox potential [21]. Oxidation of guanine moieties at carbon electrodes has been explored as a detection method in event of interaction of several compounds with DNA [22].

Fig. 3 shows the square wave voltammetric scans of the DNA biosensor before and after the interaction with Cu(II)–naringin complex. The redox behavior of native DNA exhibits two oxidation processes of guanine around 1 V (versus Ag-SPE) and adenine around 1.2 V (versus Ag-SPE) as seen in Fig. 3a. As reported by Popovich et al. [23] the rates of electron transfer between guanine or adenine and carbon electrode surface is slow and consequently the current obtained from direct oxidation of base residues is small. The contact with the complex solution affects electrochemical parameters of both nucleobases signal in a different way as can be verified in Fig. 3b. It was observed to increase in the peak current of the guanine (around 44%) with a shift of the peak potential toward more positive value (by 30 mV) than those observed for the original DNA signal. An opposite effect is observed with adenine, its signal was lower in comparison to the original DNA signal (around 34%) with a positive shift (by 20 mV) in the peak potential. These changes show that interaction between Cu(II)–naringin complex and DNA take place.

The reproducibility of the measurements was verified and each experiment was repeated at least three times on different

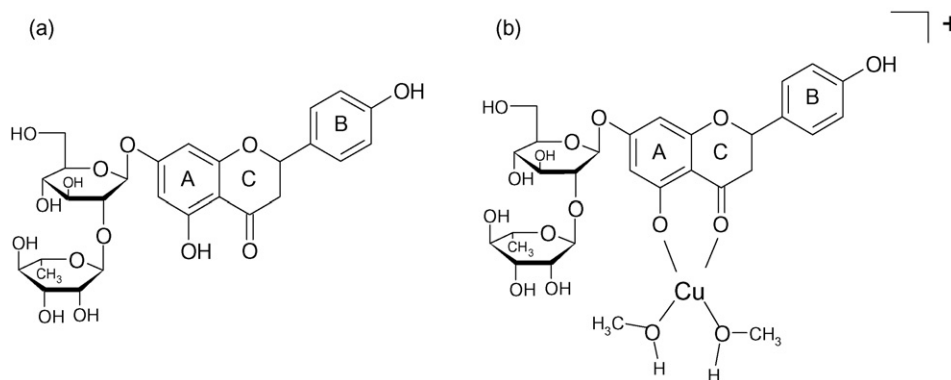


Fig. 2. (a) Structure of naringin and (b) proposed structure for the Cu(II)–naringin complex.

electrodes. The results were reproducible, leading to relative standard deviation (R.S.D.) of less than 10%.

In order to obtain more information about the interaction event, the complex was tested with a biosensor based on immobilized ssDNA and the results were compared with biosensor based on dsDNA and are shown in Fig. 4. The behavior of ssDNA biosensor was the same in both concentrations of tested complex. The signal corresponding to bases in the ssDNA biosensor was not significantly affected by the presence of the complex as indicated by the guanine response that remained almost constant, while the adenine response had a small decrease. The dsDNA biosensor signal had a great variation as a result of the contact with the complex. The observed increase in the peak current response of the bases indicates that the interaction can occur by intercalation. In fact, as reported, flavonoids are well known to be intercalators into the double stranded DNA [24–26]. Thus, the increase in the bases signal, in special the guanine signal,

due to dsDNA interaction with Cu(II)–naringin complex leading to the changes in the surface accessibility of the bases to the electrochemical oxidation process, means that the insertion of the complex into structure of DNA promotes a certain degree of opening of the double helix. It can be followed by disruption of the some hydrogen bonds between Watson–Crick base-pairs and as a result, discharging other groups in the guanine moiety to oxidize on electrode surface and consequently generating an increase in the signal.

The interaction of free naringin with DNA was not observed, however the presence of Cu(II) ion, in the complex, capable of interacting with nitrogen bases, is responsible for the interaction of the complex.

The binding of the Cu(II)–naringin complex to dsDNA is dependent on the incubation time. The effect of the accumulation time of the complex on the DNA biosensor surface was verified as shown in Fig. 5, having great influence on the guanine peak that increased with the accumulation time, whereas the adenine

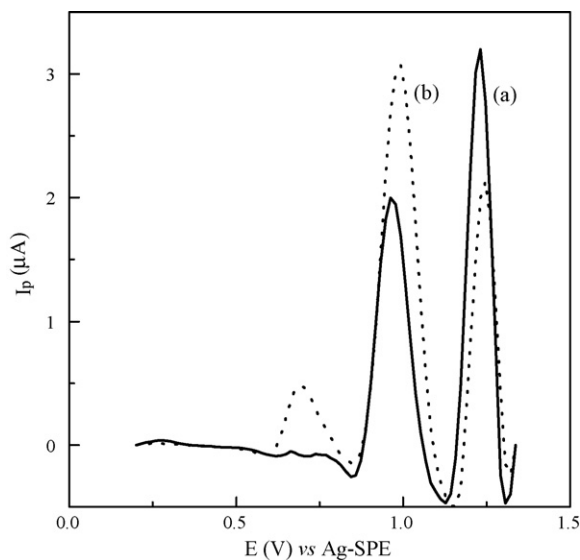


Fig. 3. SWV curves of the dsDNA-based biosensor obtained in  $0.25 \text{ mol L}^{-1}$  acetate buffer (pH 5.0) with  $10 \text{ mmol L}^{-1}$  KCl in the absence (a) (—) and presence (b) (···) of the Cu(II)–naringin complex solution  $10 \text{ mg L}^{-1}$ . SWV parameters: potential range =  $+0.2$ – $1.5 \text{ V}$ ; frequency =  $200 \text{ Hz}$ ; step potential =  $15 \text{ mV}$ ; amplitude potential =  $40 \text{ mV}$ . Immersion time of the electrode in the complex solution =  $30 \text{ s}$ . dsDNA solution concentration used at the immobilization =  $30 \text{ mg L}^{-1}$ .

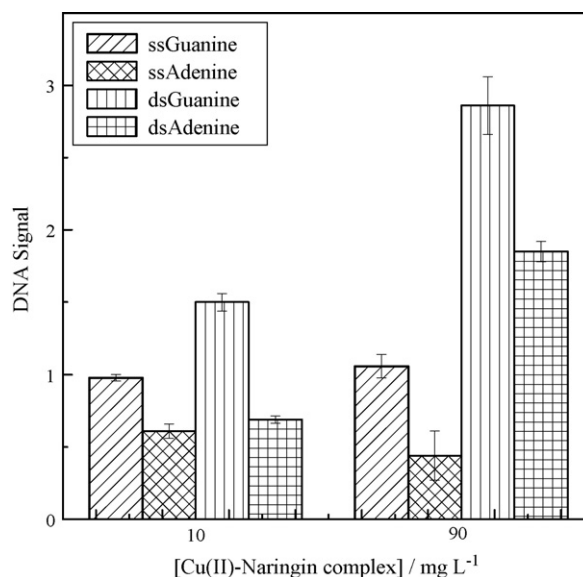


Fig. 4. Relative signals for ssDNA and dsDNA immobilized on SPE electrode surface obtained in acetate buffer solution  $0.25 \text{ mol L}^{-1}$  (pH 5.0) after the interaction with the Cu(II)–naringin complex solution. ssDNA solution and dsDNA solution concentration used at the immobilization =  $30 \text{ mg L}^{-1}$ . Other conditions as in Fig. 3.

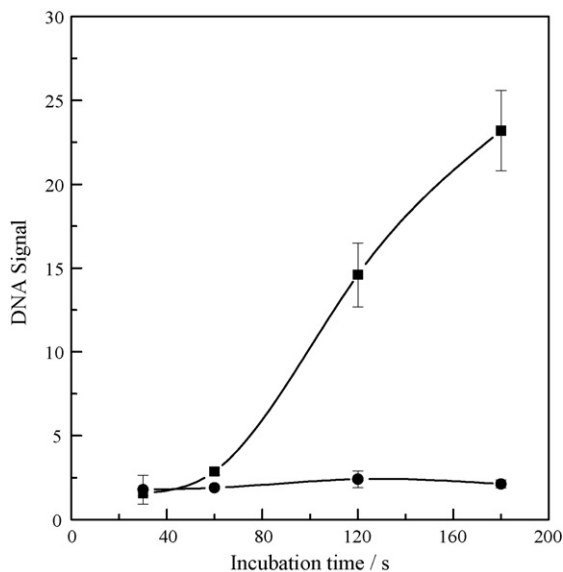


Fig. 5. Effect of the incubation time of the Cu(II)-naringin complex solution on the signal of the DNA-based biosensor related to the bases signal, (■) guanine and (●) adenine. Complex solution concentration =  $90 \text{ mg L}^{-1}$ . Other conditions as in Fig. 3.

peak showed no modification. This phenomenon demonstrates that a large contact time of the Cu(II)-naringin complex with the DNA bases probably provokes damage to guanine. These are preliminary observations and a more extensive study would be necessary in order to assert that the complex acts as cleavage agent.

### 3.3. Spectroscopic characterization of the interaction

#### 3.3.1. UV spectroscopy

Electronic absorption spectroscopy is very suitable to interaction studies related to DNA. In this sense, in Fig. 6 the UV-vis spectra of the Cu(II)-naringin complex and dsDNA in acetate buffer in the range 190–450 nm are presented. The solution of dsDNA exhibits a typical main absorption band at 260 nm, while flavonoid modified with Cu(II) in buffer solution shows a small and large band at 350 nm. The very small absorption of Cu(II)-naringin complex might be explained by its very low solubility in aqueous solvent. The spectrum of the mixed solution exhibits only a maximum absorption band common to dsDNA close to its absorption region (around 260 nm). This can be justified considering that the intermolecular bonds formed between DNA and complex resulted in a decrease in the bond order and led the low energy electronic transition [27]. This result is a typical characteristic of intercalation mode [26,28] involving a strong stacking interaction between the aromatic chromophore region of the complex and the base-pairs of DNA.

#### 3.3.2. CD spectroscopy

The type of interaction is also confirmed by circular dichroism experiments as shown in Fig. 7: the spectra of DNA in the absence (Fig. 7a) and the presence of Cu(II)-naringin complex (Fig. 7b and c). A positive peak near 275 nm and a negative peaks

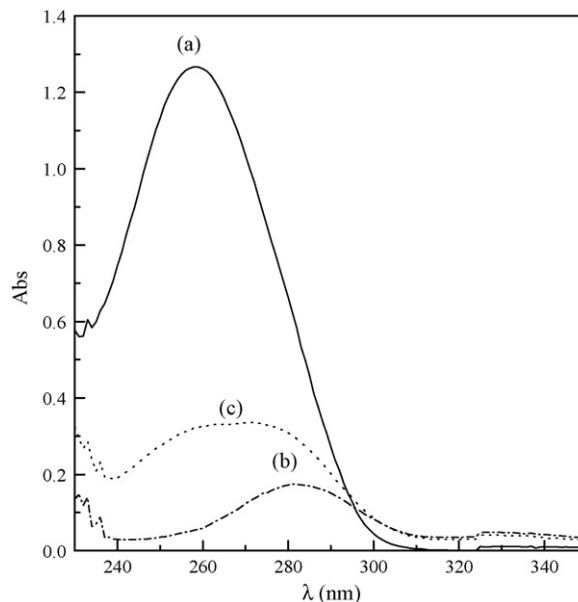


Fig. 6. UV spectra obtained in  $0.25 \text{ mol L}^{-1}$  (pH 5.0) acetate buffer solution for (a)  $25 \text{ mg L}^{-1}$  dsDNA solution, (b)  $2.5 \text{ mg L}^{-1}$  Cu(II)-naringin complex solution and (c) mixture of dsDNA and Cu(II)-naringin complex solutions.

around 246 nm can be visualized. The negative spectrum corresponds to the helical structure of DNA (helicity) and the positive spectrum corresponds to stacking of the base-pair that is characteristic of DNA in the right-handed B form [29,30]. The presence of the Cu(II)-naringin complex does not affect in a significant way the profile of the CD spectrum of DNA. A decrease in the absorption intensity of both positive and negative bands in the CD spectra is observed proportional to the increase in the concentration of the complex in the dsDNA solution. These results suggest that during the binding of the complex with DNA a slight

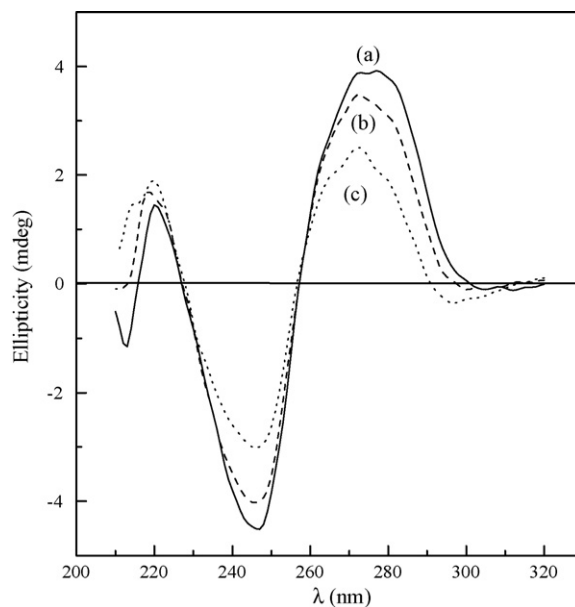


Fig. 7. CD spectra of dsDNA solution  $200 \text{ mg L}^{-1}$  (pH 5.0). (a) absence, (b) presence of  $20 \text{ mg L}^{-1}$  Cu(II)-naringin complex and (c) presence of  $50 \text{ mg L}^{-1}$  Cu(II)-naringin complex.

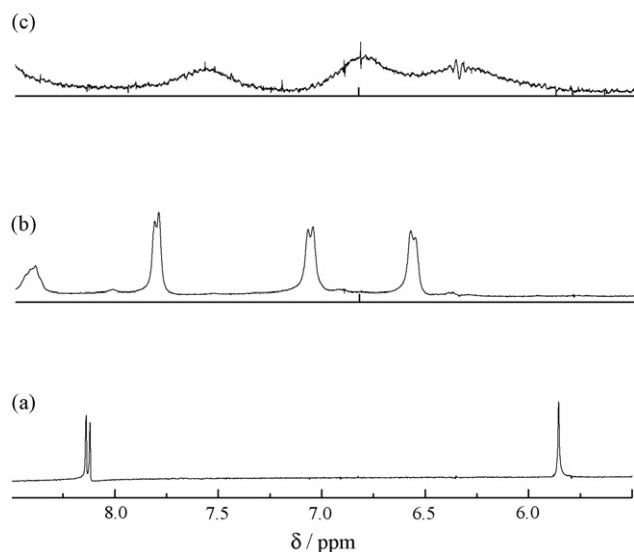


Fig. 8.  $^1\text{H}$  NMR spectra at 25 °C: (a) 5'GMP in  $\text{D}_2\text{O}$ , (b) Cu(II)-naringin complex in DMSO and (c) mixture of the 5'GMP and Cu(II)-naringin complex in  $\text{D}_2\text{O}$ . The concentration of 5'GMP and Cu(II)-naringin complex solutions were  $5.1 \times 10^{-5} \text{ mol L}^{-1}$  and  $1.8 \times 10^{-5} \text{ mol L}^{-1}$ , respectively.

change in its secondary structure occurs. In this present conditions of pH and DNA/Complex ratio for CD measurements, is possible to describe the interaction by two binding modes: the complex binds directly to DNA by base-pair type a partial intercalative interaction, which is observed by reduction in the intensity of positive band and also the interaction can take place by random surface binding inducing some partial change in the DNA conformation observed by alteration in the intensity of the negative band [31]. Probably in solution, the metal ion of the complex can interact with negatively charged phosphate groups in the surrounding DNA. Furthermore, the interaction of the complex with DNA via hydrogen bonds may help stabilize the interaction.

### 3.3.3. $^1\text{H}$ NMR spectroscopy

Using the  $^1\text{H}$  NMR spectroscopy and evaluating the changes in the chemical shifts of the protons is possible to obtain specific information about the interaction sites. As reported, intercalator compounds are investigated and related to their biological activity involving coordination to DNA preferentially by base residues in single or double-stranded DNA usually with adduct formation [32]. Binding sites are N7 of guanine, N7 and N1 of adenine and N3 of cytosine [33]. In our case, the interaction was evaluated by decrease of the protons signal of the guanine and the appearance of these signals corresponding to guanine bound to Cu(II)-naringin complex.

The reaction of 5'GMP and the Cu(II)-naringin complex was monitored by  $^1\text{H}$  NMR spectroscopy as displayed in Fig. 8. In Fig. 8a the signal of H8 of 5'GMP at  $\delta$  8.18 was observed, when the complex was mixed with 5'GMP a new signal of H8 went downfield ( $\delta$  7.63), proving the interaction via N7 of 5'GMP [34]. After 24 h a new  $^1\text{H}$  NMR spectrum was obtained and no change was observed in the proton signal indicating that interaction is stable (data not shown).

As shown in the  $^1\text{H}$  NMR spectra, the downfield displacement of the H(8) proton of 5'GMP, indicated that the coordination site of Cu(II)-naringin complex to DNA occurred via N(7) of guanine (Fig. 8c). The NMR information confirms the proposition that the Cu(II)-naringin complex acts as an intercalator, binding to DNA preferentially by guanine residues instead of the DNA phosphate groups.

## 4. Conclusions

The results of this work demonstrated the interaction of the Cu(II)-naringin complex with DNA by electrochemical and spectroscopic methods. The binding of Cu(II)-naringin complex to DNA resulted in changes in the electrochemical behavior of the purine bases, which suggested that the interaction takes place. The changes in the spectroscopic characteristics of DNA and Cu(II)-naringin complex in aqueous medium, measured by UV and circular dichroism, indicated that the predominant interaction mode may be by intercalation. The information from  $^1\text{H}$  NMR spectra corroborated to the nature of the interaction demonstrating that the coordination of the Cu(II)-naringin complex to dsDNA probably occurs via N(7) of the guanine. However, the presence of hydroxide groups in the flavonoid portion could provide interaction with DNA via hydrogen bonds, stabilizing the interaction between the complex and DNA. The electrostatic interaction with phosphate groups cannot be discarded either.

## Acknowledgements

The authors are grateful to FAPESP and CNPq for the financial support.

## References

- [1] S. Rauf, J.J. Gooding, K. Akhtar, M.A. Ghauri, M. Rahman, M.A. Anwar, A.M. Khalid, *J. Pharm. Biomed. Anal.* 37 (2005) 205–217.
- [2] V. Brabec, J. Kasparkova, *Drug Resist. Update* 8 (2005) 131–146.
- [3] J. Kang, Z. Li, X. Lu, *J. Pharm. Biomed. Anal.* 40 (2006) 1166–1171.
- [4] R. Solimani, *Biochem. Biophys. Acta* 1336 (1997) 281–294.
- [5] S. Bi, C. Qiao, D. Song, Y. Tian, D. Gao, Y. Sun, H. Zhang, *Sens. Actuators B* 119 (2006) 199–208.
- [6] S. Usha, I.M. Johnson, R. Malathi, *J. Biochem. Mol. Biol.* 38 (2005) 198–205.
- [7] S. Usha, I.M. Johnson, R. Malathi, *Mol. Cell. Biochem.* 284 (2006) 57–64.
- [8] M.G. Alvarez, G. Alzuet, J.L.G. Gimenez, B. Macias, J. Borrás, *Z. Anorg. Allg. Chem.* 631 (2005) 2181–2187.
- [9] K. Fukuhara, N. Miyata, *Bioorg. Med. Chem. Lett.* 8 (1998) 87–92.
- [10] Y. Ohshima, S. Yoshie, S. Auriol, I. Gilibert, *Free Radic. Biol. Med.* 25 (1998) 1057–1065.
- [11] F. Hayakawa, T. Kimura, T. Maeda, M. Fujita, H. Sohmiya, M. Fujii, T. Ando, *Biochem. Biophys. Acta* 1336 (1997) 123–131.
- [12] M. Johnson, G. Loo, *Mutat. Res.* 459 (2000) 211–218.
- [13] Rahman, H.S.M. Shahabuddin, J.H. Parish, K. Ailney, *Carcinogenesis* 10 (1989) 1833–1839.
- [14] M.S. Ahmed, V. Ramesh, V. Nagaraja, J.H. Parish, S.M. Hadi, *Mutagenesis* 9 (1994) 193–197.
- [15] D. Ozkan, H. Karadeniz, A. Erdem, M. Mascini, M. Ozsoz, *J. Pharm. Biomed. Anal.* 35 (2004) 905–912.
- [16] M.E. Rice, Z. Galus, R.N. Adams, *J. Electroanal. Chem.* 143 (1983) 89–102.

- [17] G. Yogeewaran, P. Viswanathan, V. Sriram, *J. Agric. Food Chem.* 48 (2000) 2802–2806.
- [18] W.F. De Giovanni, R.F.V. Souza, *Spectrochim. Acta A* 61 (2005) 1985–1990.
- [19] R.M.S. Pereira, N.E.D. Andrade, N. Paulino, A.C.H.F. Sawaya, M.N. Eberlin, M.C. Marcucci, G.M. Favero, E.M. Novak, S.P. Bydlowski, *Molecules* 12 (2007) 1352–1366.
- [20] L.D. Mello, S. Hernandez, G. Marrazza, M. Mascini, L.T. Kubota, *Biosens. Bioelectron.* 21 (2006) 1374–1382.
- [21] S. Steenken, *Chem. Rev.* 89 (1989) 503–520.
- [22] M. Mascini, I. Palchetti, G. Marrazza, *Fresen. J. Anal. Chem.* 369 (2001) 15–22.
- [23] N.D. Popovich, A.E. Eckhardt, J.C. Mikulecky, M.E. Napier, R.S. Thomas, *Talanta* 56 (2002) 821–828.
- [24] A.J. Bard, M.T. Carter, M. Rodriguez, *J. Am. Chem. Soc.* 111 (1989) 8901–8911.
- [25] Z. Zhu, C. Li, N.Q. Li, *Microchem. J.* 71 (2002) 57–63.
- [26] A.M.O. Brett, V. Diculescu, *Bioelectrochemistry* 64 (2004) 143–150.
- [27] E. Seibert, A.S. Chin, W. Pfeleiderer, *J. Phys. Chem. A* 107 (2003) 178–185.
- [28] E.C. Long, J.K. Barton, *Acc. Chem. Res.* 23 (1990) 273–279.
- [29] Rich, A. Nordheim, A.H.J. Wang, *Annu. Rev. Biochem.* 53 (1984) 791–843.
- [30] Y.M. Song, X.R. Zheng, X.Q. Yao, *Trans. Met. Chem.* 31 (2006) 616–620.
- [31] B. Selvakumar, V. Rajendiran, P.U. Maheswari, H. Stoeckli-Evans, M. Palaniandavar, *J. Inorg. Biochem.* 100 (2006) 316–330.
- [32] J.M. Sequaris, E. Kaglin, B. Malfoy, *FEBS Lett.* 173 (1984) 95–98.
- [33] J. Swiatek, *J. Coordin. Chem.* 33 (1994) 191–217.
- [34] M.A. Martinez, S. Moradell, J. Lorenzo, A. Rovira, M.S. Robillard, F.X. Avilés, V. Moreno, R. Llores, J. Reedijk, A. Llobet, *J. Inorg. Biochem.* 96 (2003) 493–502.